Membrane Currents Examined under Voltage Clamp in Cultured Neuroblastoma Cells

Abstract. *Examination of ionic membrane currents in a voltage-clamped neuronal cell line derived from the mouse C1300 neuroblastoma disclosed four kinetically different components: sodium, potassium, calcium, and leakage current. The kinetics, voltage dependence, and pharmacological properties of the sodium and potassium currents qualitatively resemble those of the corresponding currents in squid giant axon and frog myelinated nerve fiber, suggesting that the molecular structures of the sodium and potassium channels in neuroblastoma are similar to those of the nonmammalian preparations.*

Much insight into the behavior of excitable membranes has been gained from voltage-clamp studies of nonmammalian preparations such as squid giant axon and amphibian myelinated nerve fiber (*1*). The lack of a suitable system has, however, hampered the application of this powerful technique to the study of membrane excitability in mammalian nerve cells and of the development of ionic conductance mechanisms during differentiation of excitable cells. Recent advances in tissue culture techniques and especially the establishment of cell lines from the mouse C1300 neuroblastoma provide a system with advantages for investigating these questions. These cell lines express many neuronal properties and have been used extensively as a model system to explore various aspects of neuronal differentiation (*2*). Confluent cells of the adrenergic clone N1E-115 (*3*), in particular, show a high degree of morphological differentiation when grown in the presence of dimethylsulfoxide (DMSO) (*4*). These differentiated cells possess electrical properties similar to those found in normal nerve cells (*4*) and are large enough to permit stable penetration by two microelectrodes. Previous electrophysiological studies have revealed that in addition to a tetrodotoxin (TTX)-sensitive sodium current, a small calcium current is involved in the generation of the neuroblastoma action potential (*5*). However, since only the membrane potential has been examined, our knowledge concerning the ionic membrane currents underlying electric excitability in neuroblastoma is indirect and rather limited. Successful application of the voltage-clamp technique is, therefore, essential for further analysis of the physiological properties of neuroblastoma cells. In the experiments reported here we recorded membrane currents in voltage-clamped differentiated N1E-115 cells and showed that the total ionic membrane currents comprise four kinetically different components: sodium, potassium, calcium, and leakage current, each of which exhibits many of the features of the corresponding currents in nonmammalian excitable cells.

The N1E-115 cultures (*6*) were grown to confluence in Dulbecco's modified Eagle's medium (90 percent by volume) containing 14.4 m*M* $NaHCO_3$, supplemented with fetal calf serum (10 percent by volume) (Gibco), at 37°C in an atmosphere of 5 percent CO_2 in air. To obtain differentiated cells, cultures were maintained in confluence for at least 3 to 4 weeks and subsequently replated at a density of 5×10^5 cells per 60-mm dish in growth medium containing 1 to 2 percent DMSO, as described previously (*4*). Electrophysiological experiments were performed 1 to 2 weeks after replating, when cells displayed well-developed electrical excitability (the maximum rate of rise of the action potential reached 130 volt/sec). The culture dish was held in a chamber on the stage of an inverted phase-contrast microscope with control of temperature (34° to 37°C) and *p*H (7.2 to 7.4) (*7*). Cells 60 to 110 μm in diameter were impaled with two low-resistance microelectrodes (3*M* KCl, 3 to 12 megohms) arranged in an electrical circuit allowing both current and voltage clamping (*8*). Constant-current stimulation of the cells through one electrode (arranged in a bridge circuit) always gave rise to identical voltage responses at both electrodes, indicating that the membrane potential in the cell soma is spatially uniform. However, under voltage-clamp conditions, cells with long processes often exhibited delayed all-or-none inward currents. These spurious current patterns, which indicate action potential generation in regions not under voltage control, were not observed in cells with processes shorter than 200 μm. To ensure reliable space clamping we therefore selected cells without processes or with processes no longer than 200 μm.

Figure 1A shows a series of typical membrane currents recorded at depolarizing voltage steps from a holding potential of −85 mv (*9*) to various levels. During depolarization of up to −35 mv the initial capacitive current, which lasted only 0.3 msec in this experiment, was followed by a small ohmic leakage current. When the membrane potential was stepped to levels more positive than −35 mv, transient inward currents appeared, showing fast activation and inactivation kinetics. At depolarizations larger than 0 mv, activation of the inward currents was partially obscured by the tail of the capacitive current, indicating that the time for the maximum inward current to reach its peak was less than 0.3 msec. This hampered precise determination of the reversal potential of the fast current. The reversal potential, which was 30 to 40 mv, is, however, in the range of the equilibrium potential for sodium in neuroblastoma cells (*10*), which suggests

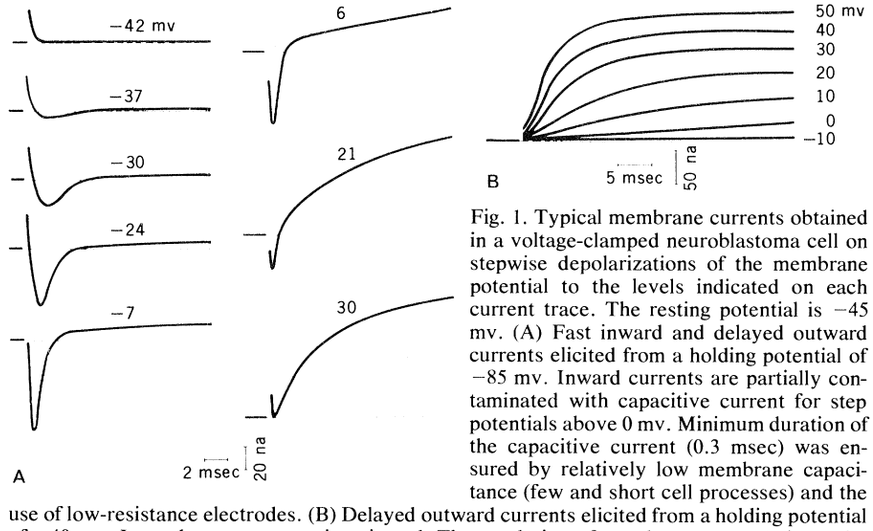

Fig. 1. Typical membrane currents obtained in a voltage-clamped neuroblastoma cell on stepwise depolarizations of the membrane potential to the levels indicated on each current trace. The resting potential is −45 mv. (A) Fast inward and delayed outward currents elicited from a holding potential of −85 mv. Inward currents are partially contaminated with capacitive current for step potentials above 0 mv. Minimum duration of the capacitive current (0.3 msec) was ensured by relatively low membrane capacitance (few and short cell processes) and the use of low-resistance electrodes. (B) Delayed outward currents elicited from a holding potential of −40 mv. Inward currents were inactivated. The resolution of membrane currents is on the order of 1 na. Membrane currents and clamp potentials were displayed on an oscilloscope and photographed. Current traces were drawn from the enlarged original records. The initial capacitive current was omitted in (B). The dashed line in each current trace refers to the zero baseline. Inward current is shown as a downward deflection.

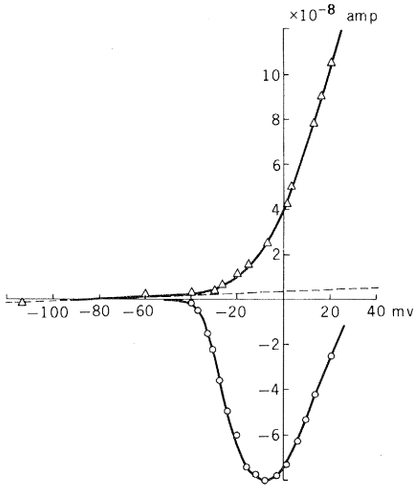

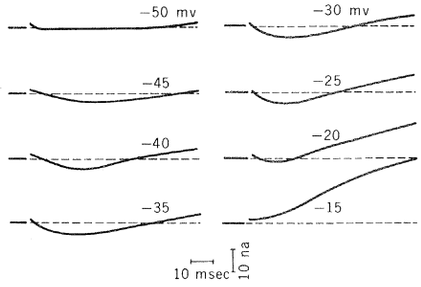

Fig. 2 (left). Current-voltage relations for peak values of net inward current (circles) and steady-state values of delayed outward current (triangles) obtained from the same cell as in Fig. 1. The holding potential was −85 mv. Steady-state values were measured at 50 msec after the onset of the clamp step. The dashed line represents leakage current. Fig. 3 (right). Slow membrane currents elicited at different levels of membrane potential in a voltage-clamped neuroblastoma cell bathed in sodium-free solution containing 10 m*M* calcium (sodium chloride was isosmotically replaced by tris-Cl). The holding potential was −80 mv. Delayed outward current can be seen with depolarizations beyond −25 mv. Current traces were drawn as in Fig. 1.

that sodium is the main charge carrier for the fast current. The fast current was inactivated within 5 msec and was followed by delayed outward currents, which are seen clearly at clamp potentials above 0 mv. When the inward currents had been completely inactivated by setting the holding potential at −40 to −30 mv, depolarizing steps to various levels produced only delayed outward currents, as shown in Fig. 1B. The outward currents rose to a plateau along a voltage-dependent S-shaped curve with a much slower time course (5 to 50 msec). The reversal potential of the delayed current was determined from an analysis of the tail currents recorded on stepping the membrane potential to different levels at the end of a depolarizing pulse. The values obtained (−65 to −85 mv) are close to the equilibrium potential for potassium in neuroblastoma cells (*10*), which suggests that the outward currents are carried primarily by potassium.

The peak values of the net inward current, the steady-state values of the delayed outward current, and the leakage current are plotted as a function of clamp potential in Fig. 2. These current-voltage relations closely resemble those of extensively studied nonmammalian preparations. Thus, while the leakage current is a linear function of the voltage, the steady-state current displays a distinct rectification and the peak transient current develops a characteristic negative resistance region between −45 and about −5 mv. The transition from the resting membrane conductance to a higher conductance in this membrane potential range marks the threshold for generation of the neuroblastoma action potential.

To determine the contribution of sodium to the fast inward current, we added TTX to the bathing medium. At a concentration of 10^{-6} g/ml, TTX completely abolished the fast current. The same effect was obtained when external sodium was replaced by tris (hydroxymethyl)methylamine (tris). This is convincing evidence that sodium is the only charge carrier for the fast inward current. Similarly, in a solution containing 15 m*M* tetraethylammonium ions to inhibit the potassium current, about 80 percent of the delayed outward current was eliminated. This demonstrates that the outward current is carried mainly by potassium ions.

In several experiments spherical cells without neurites were used to obtain a reliable estimate of membrane area. From these determinations the peak sodium current density was calculated to be 0.3 to 0.7 ma/cm² at 20°C. This current density is one order of magnitude smaller than the value of 8 ma/cm² reported for the squid giant axon at 20°C (*1*).

Under favorable experimental conditions (low leakage conductance and low electrode noise level) another component of inward current appeared. This current, which was very small, showed slow activation and inactivation kinetics and could be detected in sodium-free solution (tris substitution). However, measurement of this current was difficult because (i) the maximum value of the current was smaller than the value of the outward leakage current, and (ii) reproducibility under voltage clamp was poor. Both the reproducibility and the magnitude of this current were markedly enhanced when the external calcium concentration was raised from 1.8 to 10 m*M*, as illustrated in Fig. 3. In this experiment the maximum value at peak, which was 5 to 10 percent of the corresponding value of the sodium current, was reached after 15 msec, when the membrane potential was stepped to −30 mv from a holding potential of −80 mv. This slow current was not affected by TTX and could be blocked reversibly by cobalt ions (5 m*M*). These observations provide additional evidence that a separate calcium conductance system underlies the weak and slow afterdepolarization of the neuroblastoma action potential (*5*). A slow calcium current, which did not contribute to the rising phase of the action potential, was recently recorded in some molluscan neurons under voltage clamp (*11*), where it presumably regulates pacemaker activity and contributes to the activation of a calcium-sensitive potassium conductance (*12*). In the present study, however, we did not find experimental evidence for any analogous regulating role of calcium in neuroblastoma cells. Thus, the physiological significance of a voltage-sensitive calcium influx in neuroblastoma cells remains unclear.

In addition to demonstrating the feasibility of studying a clonal nerve cell line under voltage-clamp conditions, our results show that the kinetic properties, voltage dependence, and pharmacological properties of the sodium and potassium currents in neuroblastoma qualitatively resemble those of the corresponding currents in squid axon and frog node of Ranvier (*1*). This suggests that the molecular structures of the sodium and potassium channels in neuroblastoma are similar to those in the nonmammalian preparations. The neuroblastoma system therefore presents a unique opportunity to extend the voltage-clamp technique to an in vitro differentiating system which is highly suitable for biochemical analysis. This system should be of value for studying the development of ionic channels during differentiation and for characterizing molecular components that participate in ion movement through excitable membranes.

WOUTER H. MOOLENAAR*
ILAN SPECTOR
Department of Neurobiology, Weizmann Institute of Science, Rehovot, Israel

References and Notes

1. K. S. Cole, *Membranes, Ions and Impulses* (Univ. of California Press, Berkeley, 1968).
2. For reviews see F. A. McMorris, P. G. Nelson, F. H. Ruddle, *Neurosci. Res. Program Bull.* **11**, 412 (1973); G. Sato, Ed., *Tissue Culture of the Nervous System* (Plenum, New York, 1973); S. C. Haffke and N. W. Seeds, *Life Sci.* **16**, 1649 (1975); P. G. Nelson, *Physiol. Rev.* **55**, 1 (1975); K. N. Prasad, *Biol. Rev.* **50**, 129 (1975).
3. T. Amano, E. Richelson, M. Nirenberg, *Proc. Natl. Acad. Sci. U.S.A.* **69**, 258 (1972).

4. Y. Kimhi, C. Palfrey, I. Spector, Y. Barak, U. Z. Littauer, *ibid.* **73**, 462 (1976).
5. I. Spector, Y. Kimhi, P. G. Nelson, *Nature (London) New Biol.* **246**, 124 (1973).
6. The N1E-115 line was obtained from M. Nirenberg.
7. The bathing solution had the following salt concentrations (millimolar): NaCl, 109.5; KCl, 5.5; $CaCl_2$, 1.8; $MgSO_4$, 0.8; $NaHCO_3$, 14.4; and NaH_2PO_4, 1.
8. The electrical circuit was similar to that described by J. A. Connor and C. F. Stevens [*J. Physiol. (London)* **213**, 1 (1971)].
9. Cultured mouse neuroblastoma cells generally have relatively low resting potentials (−35 to −55 mv). Since membrane currents can be inactivated at these low values, the cells were kept hyperpolarized at a holding potential between −75 and −90 mv.
10. I. Spector, C. Palfrey, U. Z. Littauer, *Nature (London)* **254**, 121 (1975).
11. R. Eckert and H. D. Lux, *J. Physiol. (London)* **254**, 129 (1976).
12. R. W. Meech and N. B. Standen, *ibid.* **249**, 211 (1975).
13. Supported in part by the United States–Israel Binational Foundation. W.H.M. was supported by the Koningin Wilhelmina Fonds. We thank Y. Kimhi for supplying the differentiated cultures and D. Saya for help with the cultures.
* Permanent address: Department of Physiology, University of Leiden, Leiden, Netherlands.

30 August 1976; revised 9 November 1976

Scotopic Vision Deficits in Young Monkeys Exposed to Lead

Abstract. *Rhesus monkeys were reared on diets designed to produce blood lead concentrations of 14 (untreated), 55, or 85 micrograms per 100 milliliters for the first year of life. Eighteen months later, blood lead levels were normal in all animals. At this time, however, visual discrimination performance in the 85-microgram group was impaired under dim light relative both to their own performance under bright light and to the performance of the other groups under all light levels used. We interpret these results to reflect a deleterious, enduring impairment of scotopic visual function (night blindness) as a result of early lead intoxication.*

The sequelae of acute lead poisoning in humans and animals include visual system damage (*1*) and blindness (*2*). These effects are usually described simply as "optic atrophy" or "blurred vision" and appear only with lead poisoning severe enough to induce encephalopathy (*3*). Although it can be dramatic, lead-induced blindness is nevertheless a rare and usually transient phenomenon (*4*). Recently, some effects of subclinical (*5*) lead exposure have been described (*6*), but we are aware of no data relating visual perceptual deficits to this form of lead intoxication. We report here that rhesus monkeys exposed during infancy to subclinical levels of lead acetate, and exhibiting no overt (*7*) signs of intoxication, nevertheless manifest a deficit in scotopic vision measured 1½ years after termination of exposure to lead.

Ten rhesus monkeys were separated from their mothers at birth and reared on Similac (Ross Laboratories) in individual cages (*8*). Lead acetate was added to the Similac given to six of the animals in a daily 7 a.m. feeding of 100 ml from day 5 to day 365 post partum. Doses were adjusted to maintain target lead concentrations in whole blood at 55 μg per 100 ml in three "low-lead" monkeys, and at 85 μg in three "high-lead" monkeys; the remaining four animals served as untreated controls. Weekly midafternoon blood samples were assayed for lead concentrations (*9*). Treatment parameters and physiological responses of the three groups are shown in Table 1.

Initial lead doses averaging 0.53 mg kg^{-1} day^{-1} elevated the blood lead levels of the low-lead group to 55 μg per 100 ml by 4 weeks, after which appropriate dose adjustments were made to maintain that level. In contrast, initial doses averaging 1.15 mg kg^{-1} day^{-1} raised the blood lead levels of the three high-lead subjects to 137, 152, and 300 μg per 100 ml by 6, 9, and 5 weeks of age, respectively (*10*). With subsequent modifications of dose, these peak levels declined to near the 85 μg per 100 ml chronic target level over the next 6 to 8 weeks (*11*) and remained at that level for the rest of the treatment year.

The present experiments began 18 months after termination of lead treatment. At this time mean blood lead concentrations (in micrograms per 100 ml) were essentially normal (*12*) for all groups, with means ± standard errors of 13.50 ± 1.45 (control), 19.75 ± 5.04 (low-lead), and 22.67 ± 4.02 (high-lead). Funduscopic examination revealed no indication of optic atrophy or other observable retinal damage in any animal.

A semiautomatic Wisconsin General Test Apparatus (*13*) was equipped with eight 100-watt incandescent lamps whose brightness was controlled by a voltage regulator. Prior experiments had adapted all animals to the apparatus and to the discrimination procedure employed here. On each trial, two planometric stimuli were presented, each covering a food well located 32.5 cm from a second identical well and 3.2 cm behind the raised front edge of a gray test tray. A trial began when an opaque screen was lowered, revealing to the monkey the test tray with the two stimulus plaques lying flat upon it. The animal responded by pushing aside just one of the plaques, uncovering either a food reward in the well under the correct stimulus or an empty food well under the incorrect one. The opaque screen was then interposed, the next trial set up, and the process repeated, 50 trials per session. Subjects were tested once per day and had been fasted for 17 to 24 hours at the time of testing. The stimuli consisted of a set of six tagboard cards, 7.62 cm square, upon which were mounted photographically reproduced, black-on-white Landolt rings, 3.81-cm outside diameter and 1.90-cm inside diameter, with gap widths of 7.5 (A), 3.75 (B), 1.0 (C), 0.4 (D), and 0.0 mm (Standard); a protective transparent polyester film was laminated over the stimuli for durability. The sixth stimulus was a duplicate Standard (St+) which was always associated with reinforcement. Several stimulus sets were

Table 1. Summary of treatment parameters and physiological responses of animals during the year of exposure to lead acetate. Values shown are group means and ranges of individual animal averages for the treatment year, with the exception of body weights, which were obtained at the end of the year. All values (except those of lead consumption and blood lead concentrations) fall within normal limits for infant monkeys.

Group	Lead consumption (mg kg^{-1} day^{-1})	Blood lead conc. (μg/100 ml)	Hemoglobin (g/100 ml)	Hematocrit (%)	Blood total protein (g/100 ml)	Albumin/ globulin ratio	Similac intake (ml kg^{-1} day^{-1})	Body weight (kg)
Control	No lead	14 (10 to 20)	13.1 (12.7 to 13.6)	40.2 (38 to 42)	6.7 (6.4 to 6.9)	1.35 (1.32 to 1.43)	309 (305 to 315)	1.92 (1.7 to 2.2)
Low-lead	0.326 (0.313 to 0.346)	55 (44 to 62)	12.6 (12.2 to 13.3)	38.3 (37 to 40)	5.77 (5.6 to 6.0)	1.75 (1.59 to 2.00)	312 (310 to 315)	2.00 (1.9 to 2.1)
High-lead	1.018 (0.989 to 1.040)	85 (73 to 95)	11.8 (11.6 to 13.0)	37.5 (36 to 41)	6.33 (6.0 to 6.8)	1.72 (1.61 to 1.81)	313 (310 to 315)	1.90 (1.7 to 2.1)